



Monthly Bulletin

Institut de physique du globe de Paris
Observatoire volcanologique du Piton de la Fournaise

ISSN 2610 – 5101

February, 2026

PITON DE LA FOURNAISE (VNUM #233020)

Latitude: 21.244°S

Longitude: 55.708°E

Summit elevation: 2632 m

Piton de la Fournaise is a basaltic hot spot volcano located in the southeastern part of La Réunion Island (Indian Ocean). The volcano first erupted about 500,000 years ago. Its volcanic activity is characterized by frequent effusive eruptions (with emissions of lava fountains and lava flows) that occur on average twice a year since 1998. More rarely, larger explosive eruptions (with blocks covering the summit area and ash emissions that can disperse over long distances) have happened in the past with a centennial recurrence rate.

Most of the current eruptive activity (97% during the last 300 years) occurs from vents inside the Enclos Fouqué caldera. A few eruptions, however, have occurred from vents outside the caldera (most recently in 1977, 1986, and 1998). Such eruptions can potentially threaten communities that live in the surrounding areas.

Since late 1979, the activity of Piton de la Fournaise is monitored by the Piton de la Fournaise Volcanological Observatory (Observatoire Volcanologique du Piton de la Fournaise - OVPF), which belongs to the Institut de Physique du Globe de Paris (IPGP).

Alert level: Alerte 2-1
(from February, 13 2026)

January 27 (18h) to February 13, 2026: *Vigilance*

(cf. table in the appendix)



A. Piton de la Fournaise activity

Seismicity

The seismological network of the Piton de la Fournaise Volcanological Observatory consists of 41 seismological stations currently in operation, representing a total of 109 channels sampled at 100 Hz and transmitted in real time to the observatory. This network includes 32 three-component broadband stations, 2 three-component short-period stations and 7 analogue stations with one vertical component.

Earthquakes are located based on the arrival times of P and S waves, which are manually plotted in the SeisComP software (www.seiscomp.de) using automatic or visual detections. The earthquakes are then located using NonLinLoc software (Lomax et al., 2000), using a three-dimensional velocity model. This model takes into account a velocity gradient according to the topography and assumes a constant VP/VS ratio of 1.7. The P-wave velocity is 3.3 km/s at the free surface and increases linearly with depth at a gradient of 0.3 s⁻¹.

Observations

In February 2026, the OVPF-IPGP recorded at Piton de La Fournaise:

- 1446 shallow volcano-tectonic earthquakes (0 to 2.5 km above sea level) below the *Bory* and *Dolomieu* summit craters;
- 44 deep earthquakes (below sea level);
- 68 long-period earthquakes;
- 417 rockfalls.

Volcano-tectonic activity beneath Piton de la Fournaise in February 2026 was marked by two seismic swarms (Figure 1, top).

- February 6-7 from 23:31 UTC to 00:05 UTC,
- February 13 from 5:25 UTC to 6:00 UTC.

The shallow volcano-tectonic earthquakes were mainly clustered during these two seismic swarms, which alone accounted for **around 62% of the earthquakes observed in February 2026**. These “seismic swarms” are interpreted as markers of **shallow magmatic injections**, reflecting magma transfers from the shallow reservoir to the surface.

The seismic swarm of **February 6-7** is located beneath the summit, along the north-western edge of the ring fault (Figures 2 and 3), a structure inherited from the collapses of the summit craters, which usually concentrates a large part of the seismicity of Piton de la Fournaise. The location of the earthquakes observed during this crisis suggests a magmatic intrusion in this sector of the edifice.

The seismic swarm of **February 13**, which led to **an eruption**, is analyzed in detail in section B of this bulletin.

In addition, **417 rockfalls** were detected during the month, mainly inside the *Dolomieu* crater, along the cliffs of the *Enclos Fouqué* caldera and of the *Cassé de la Rivière de l'Est*, and on the recently formed cone and lava flows. This type of gravitational activity is common at Piton de la Fournaise

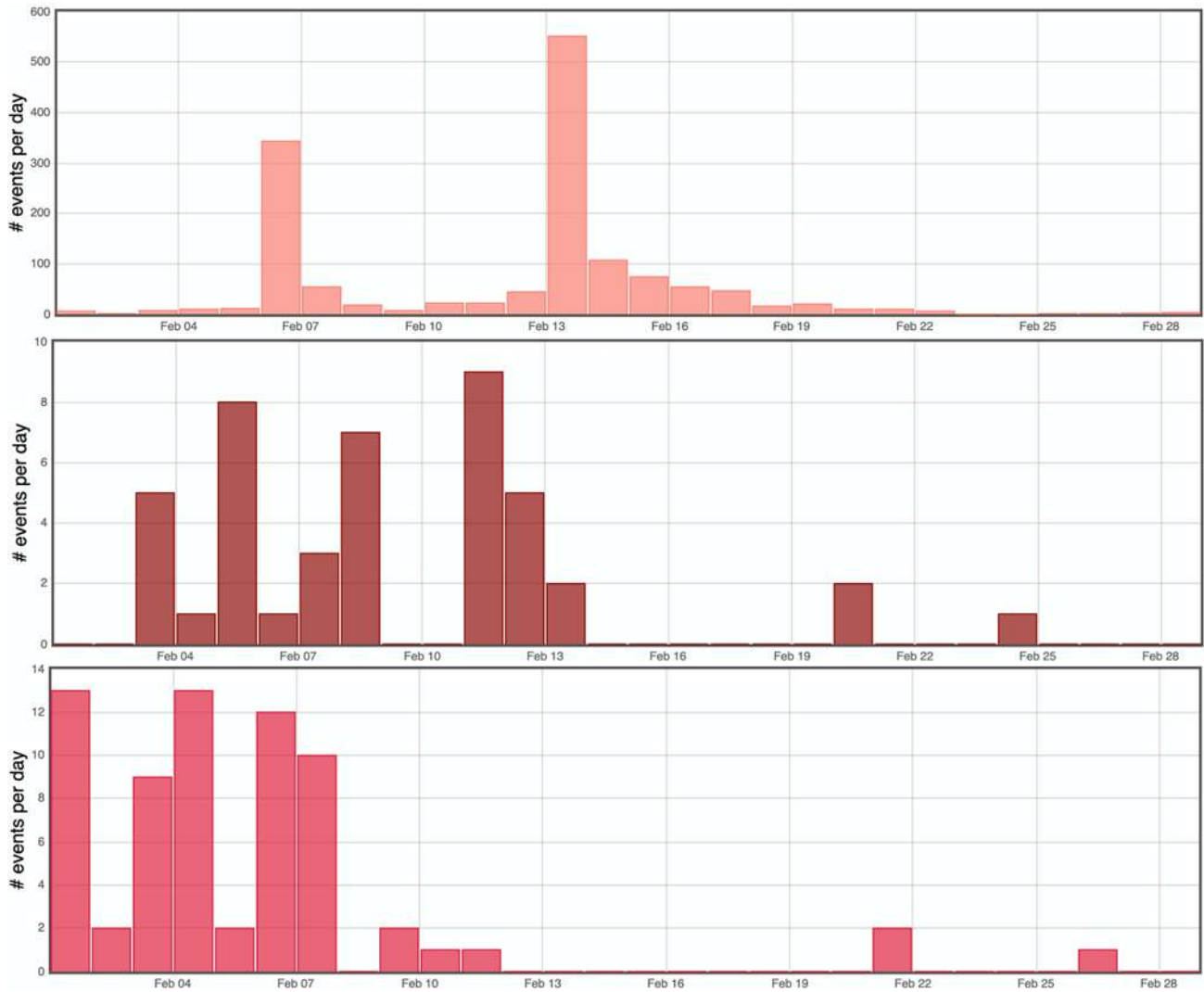


Figure 1: Number of (top) shallow volcano-tectonic, deep volcano-tectonic (middle) and long-period (bottom) earthquakes per day recorded in February 2026 (©WebObs/OVPF-IPGP).

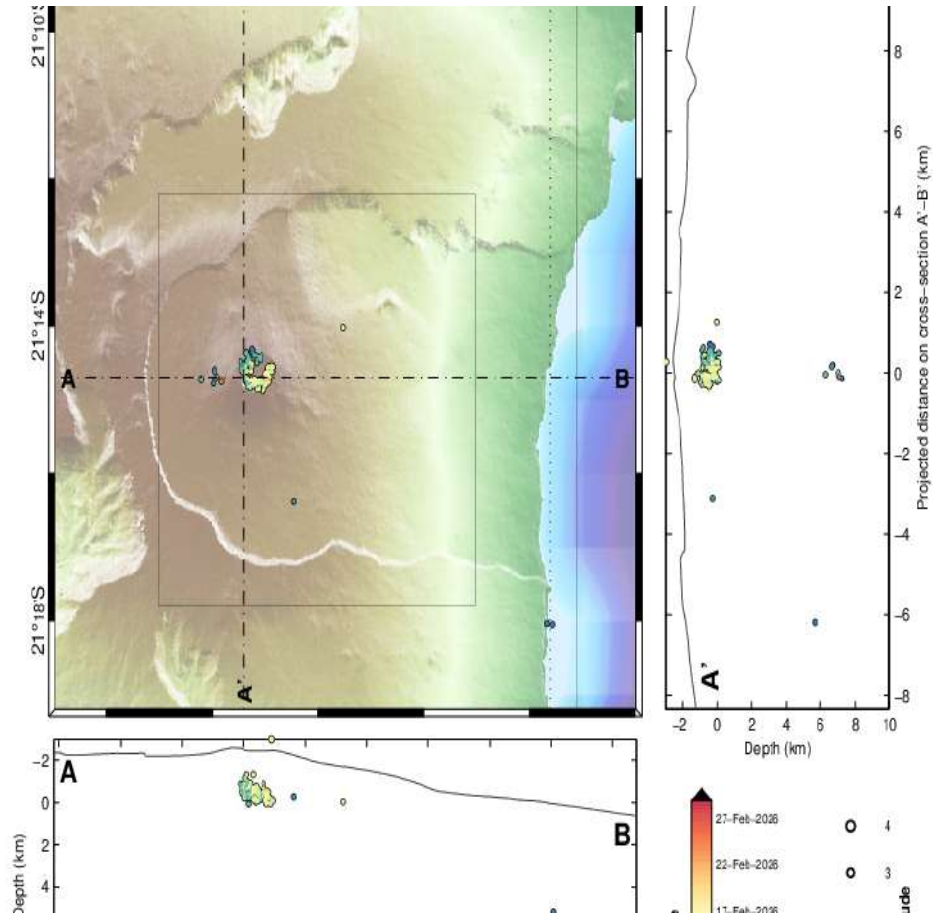


Figure 2: Seismicity below Piton de la Fournaise in February 2026. Location map (epicenters) and north-south and east-west cross-sections (hypocenters) of earthquakes as recorded by OVPF-IPGP. Only manually located earthquakes are shown on the map (©WebObs/OVPF-IPGP).

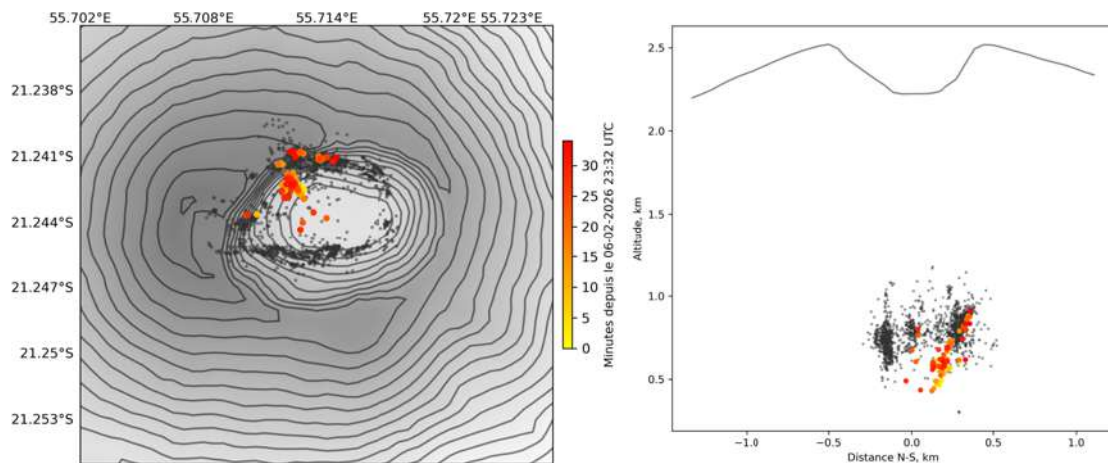


Figure 3: Seismicity recorded during the seismic swarm of February 6-7, 2026 below Piton de La Fournaise (colored according to the time since the start of the seismic swarm at 23:31 UTC). Location map (epicenters) and north-south and east-west cross-sections (showing the depth location, hypocenters) of earthquakes detected and relocated by the OVPF-IPGP. The earthquakes in black correspond to a reference catalog of shallow earthquakes since 2012 (©OVPF-IPGP).



Deformation

The permanent network for monitoring deformation at Piton de la Fournaise currently comprises:

- 27 GNSS (Global Navigation Satellite System) stations,
- 11 pairs of tiltmeters at 10 different sites,
- 3 three-component extensometers.

Once the data have been retrieved (every 15 min to every day depending on the stations), they are automatically processed using the GipsyX/JPL software (Bertiger et al., 2020; Murphy et al., 2024).

These calculations incorporate the new JPL products in ITRF2020 (Altamimi et al., 2023, Rebischung et al., 2024). The calculated coordinates are expressed relative to the Figure Centre (FC), a concept more suited to small-scale area of work.

Observations

Between April 2024 and November 2025, GNSS data recorded deflation of the edifice visible both at the summit zone and in the far field (Figures 4 and 5).

Since late November, a change in trend has been visible on all baselines, with the onset of an increase of the distance reflecting **inflation of the edifice**. This inflation, whose source is **shallow** (above sea level) and located **below the summit**, corresponds to the **pressurization of the volcano's shallow feeding system**. This pressurization led to intrusions on December 5 (see December 2025 monthly bulletin), January 1, 2026 (see January 2026 monthly bulletin), February 6-7, 2026, as well as the eruptions of January 18-20, 2026 (see January 2026 monthly bulletin) and the one that start on February 13, 2026 (see section B for more details).

The **February 6-7, 2026 intrusion** generated no deformation visible at the summit GNSS stations (Figures 4 and 5) but only slope variations of a few micro-radians on the tiltmeters located at the summit.

The injection of magma leading to the **eruption that start on February 23**, was accompanied by **rapid and stronger deformation** (of a few decimeters) on the southern and southeastern flanks of the terminal cone (see section B for more details).

Following the start of the eruption, summit deflation was recorded, linked to the emptying of the shallow magma reservoir feeding the eruption (Figures 4, 5, and 6).

Since the end of February, more precisely around February 21, **a slight edifice inflation** seems to be emerging, mainly at the summit GNSS stations and at the base of the terminal cone. This resumption of inflation would indicate a slight re-pressurization of the magma feeding system, possibly linked to a recharge of magma in the shallow reservoir.

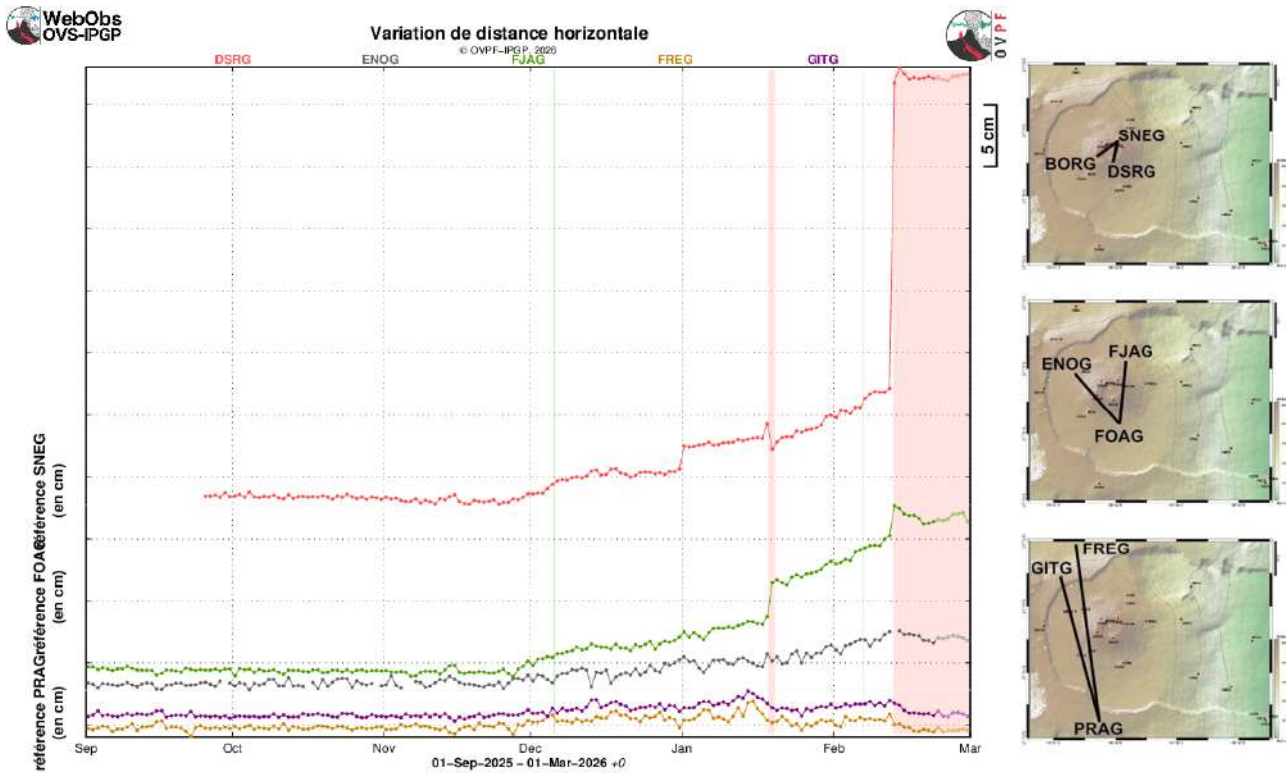


Figure 4: Ground deformation records over the past six months (the red and green bars represent eruptive and intrusive periods, respectively). The time series plots show the changes in horizontal distance between pairs of GNSS stations located around the Dolomieu summit crater (reference: SNEG; top graph), the terminal cone (reference: FOAG; middle graph) and the Enclos Fouqué caldera (reference: PRAG; bottom graph), from north to south (see location on the right). Increasing distances (or baseline elongation) indicate volcano inflation, while decreasing distances (or baseline contraction) reflect edifice deflation (©Webobs/OVPF-IPGP).

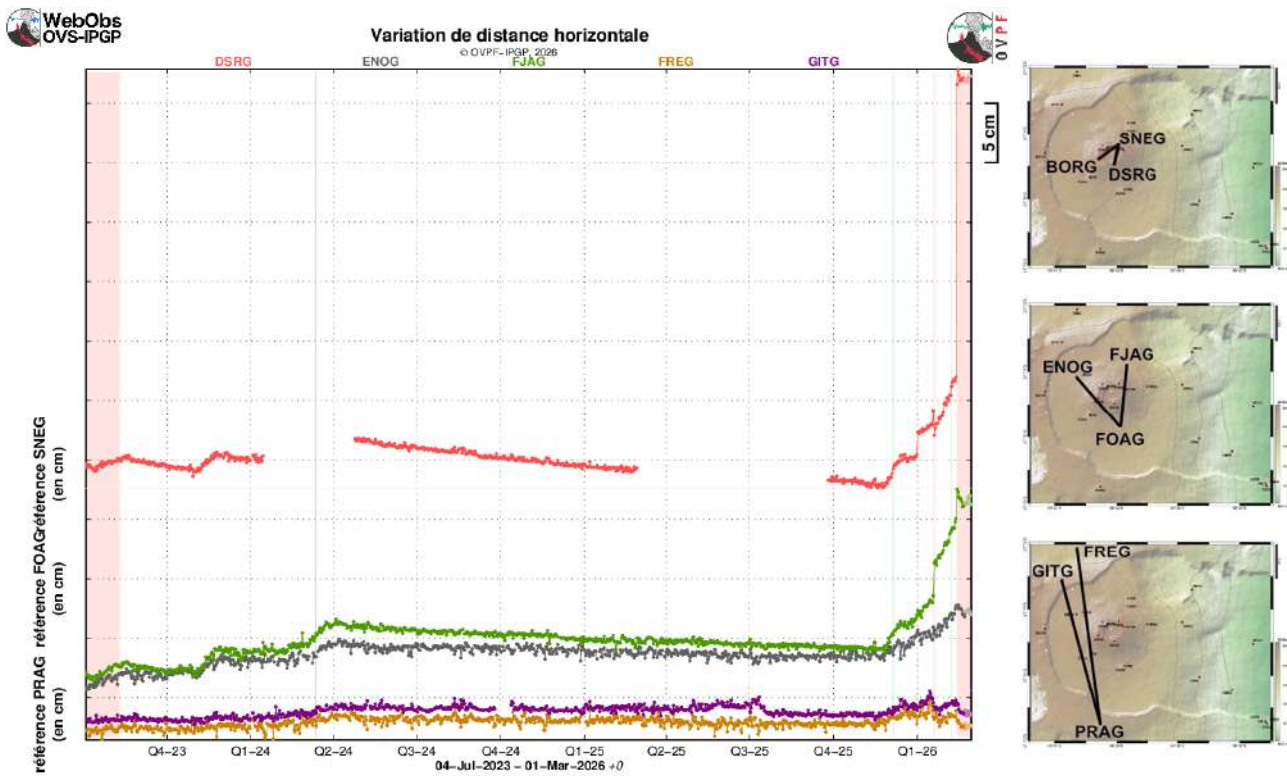


Figure 5: Ground deformation records since the eruption of July-August 2023 (the red and green bars represent eruptive and intrusive periods, respectively). The time series plots show the changes in horizontal distance between pairs of GNSS stations located around the Dolomieu summit crater (reference: SNEG; top graph), the terminal cone (reference: FOAG; middle graph) and the Enclos Fouqué caldera (reference: PRAG; bottom graph), from north to south (see location on the right). Increasing distances (or baseline elongation) indicate volcano inflation, while decreasing distances (or baseline contraction) reflect edifice deflation (©WebObs/OVPF-IPGP).

* Glossary: The summit GNSS signals indicate the influence of a shallow pressure source below the volcano, while distant GNSS signals indicate the influence of a deep pressure source below the volcano. Inflation usually means pressurization; and conversely deflation usually means depressurization.

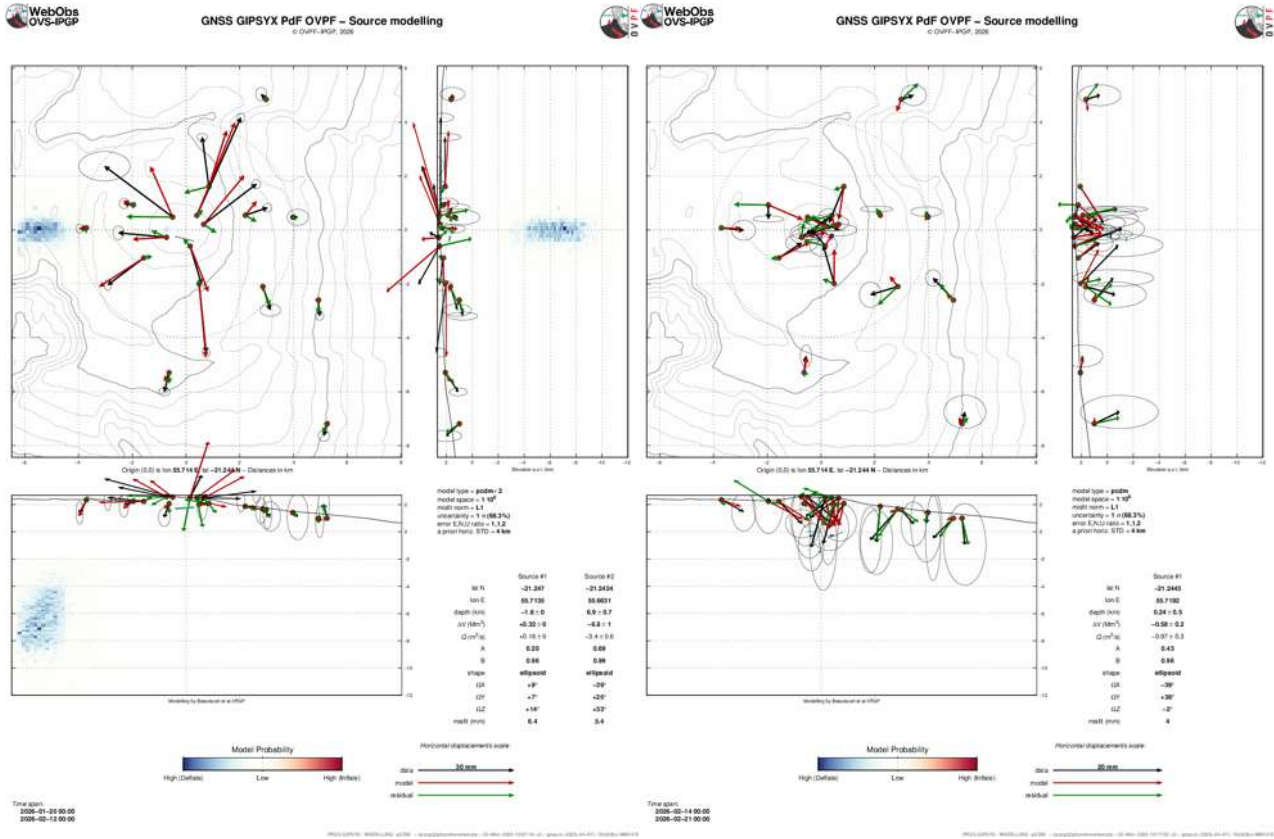


Figure 6: Modelling of the pressure sources responsible of ground displacements (pCDM models) linked (left) to the pre-eruptive period from January 20 to February 12 and (right) to the syn-eruptive period from February 14 to 21. The black vectors represent observed data, the red vectors represent modelled vectors, and the green vectors represent the residuals between observed and modelled vectors (©Webobs/OVPF-IPGP).



Gas geochemistry

The permanent geochemical network for monitoring gas emissions from Piton de la Fournaise currently comprises:

- 3 MAX-DOAS stations measuring the optical thickness of SO₂ (ppm.m) in the atmosphere. Measurements are taken every 10 to 15 minutes during the day when weather conditions are favorable (Arellano et al., 2020).
- 1 MultiGaS station measuring excess H₂O, CO₂, SO₂ and H₂S relative to the atmosphere, with measurements taken every 6 hours.
- 4 stations measuring CO₂ flux through the soil. At these stations, meteorological parameters (temperature, pressure, humidity, wind speed and direction) are also recorded in order to correct signals from environmental disturbances (Boudoire, 2017; Bénard et al., 2023). Measurements are taken every hour.

Observations

CO₂ concentration in the soil

Since the eruption of July, 2 - August, 10 2023, an overall trend of decrease in soil CO₂ emissions is recorded on most stations, associated with moderate positive pulses having minor-moderate intensity (Figure 7).

The PCRN station (OVPF site) shows a change in this trend.

In the shorter term, an upward trend is also measured at the distal BLEN station and the proximal GITN station.

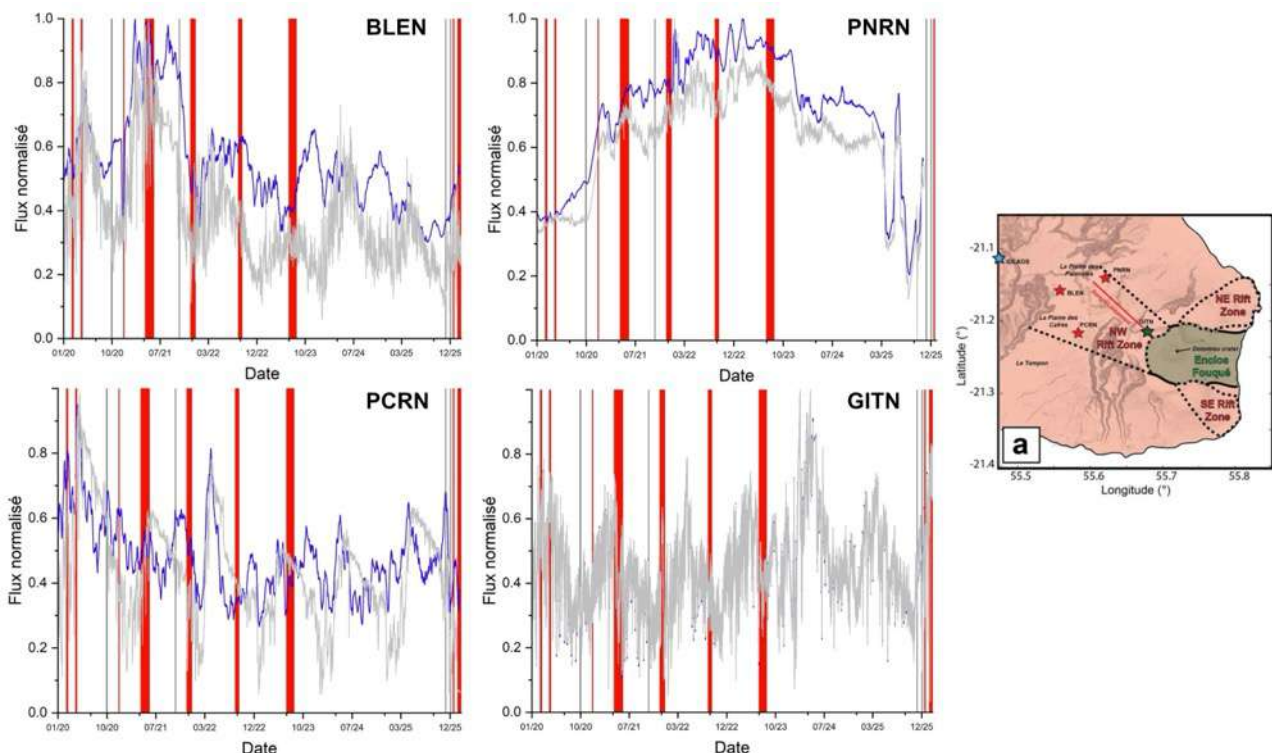


Figure 7: Normalized CO₂ soil emissions (grey: raw data) corrected for short period influence of environmental parameters (OVPF-correction model; 15 days moving average; in blue) of all CO₂ stations (see location on the map on the right). Red bars: eruptions; Gray bars: intrusions (©OVPF-IPGP-OSUL).



* Glossary: CO₂ is the first gas to be released from deep magma (rising from the mantle), so its detection in the far field often means a deep rise of magma. Its near-field evolution may be related to magmatic transfer in the shallowest part of the feeding system (< 2-4 km below the surface).

Summit fumaroles composition obtained by the MultiGas method

During volcano quiescence, MultiGaS station located at the summit of the volcano measures weak SO₂ and H₂S concentrations often close or below detection levels.

Weak concentrations of SO₂ (<0.3 ppmv) and H₂S, associated with H₂O have been recorded between November 2024 and March 2025, showing a potential weak regain in activity of the hydrothermal system.

A new phase of detection of weak SO₂ and H₂S concentration in the atmosphere at the volcano summit is recorded since November 10 2025 and has peaked in December 2025 - January 2026 during successive intrusion phases (December 5, 2025 and January 1, 2026) and during the short-lived eruption of January 18-20, 2026 (Figure 8).

Stronger concentrations (> 1ppmv) are measured during the still ongoing February 2026 eruption.

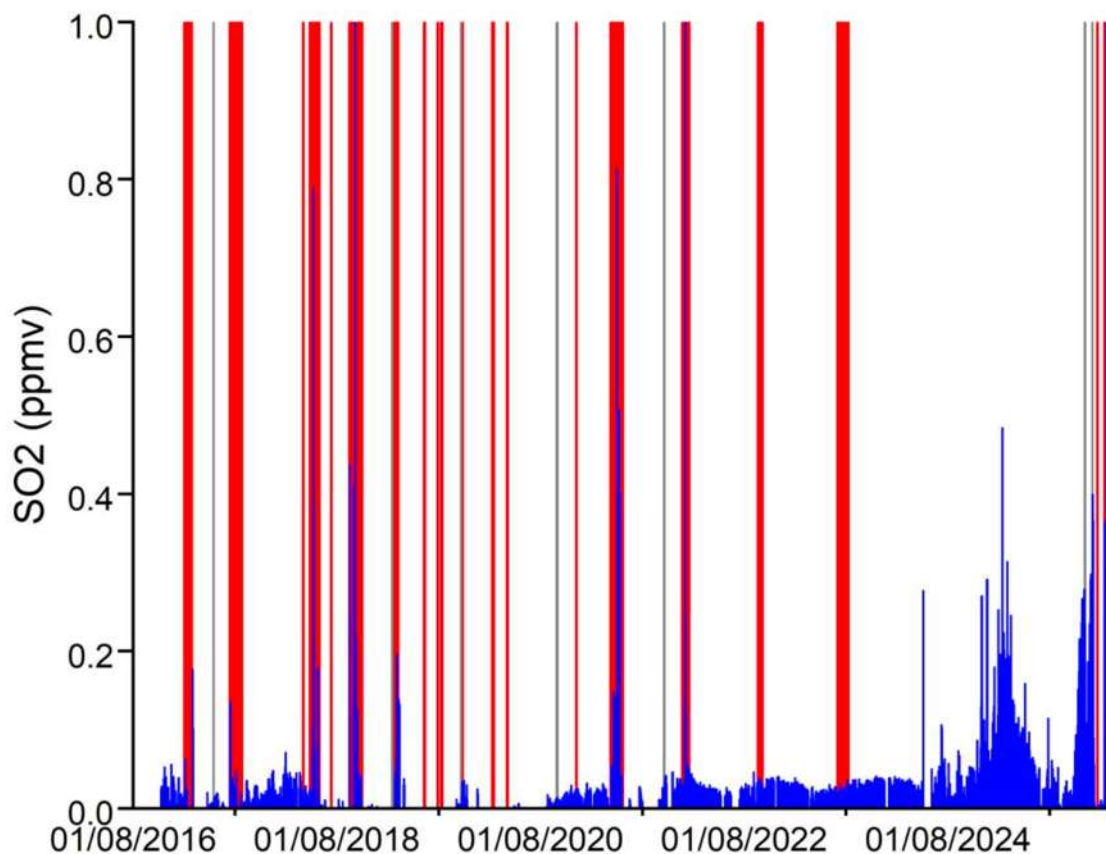


Figure 8: Raw (in blue) concentrations of SO₂ in the atmosphere at the summit of Piton de la Fournaise (MultiGaS station) Red bars: eruptions; Gray bars: intrusions (©OVPF-IPGP-OSUL).



* Glossary: The MultiGaS method allows measuring the concentrations of H₂O, H₂S, SO₂ and CO₂ in the atmosphere at the summit of the Piton de la Fournaise volcano. Magmatic transfer in the Piton de la Fournaise feeding system can result in an increase in SO₂ concentrations and in the C/S ratio (carbon/sulfur).

SO₂ flux in the air obtained by DOAS method

The NOVAC stations located on the edges of the Enclos Fouqué (“Enclos0” to the west, “Piton de Bert” to the south, and “Piton Partage” to the north) detected the gas plume associated with the eruption that start on February 13, 2026.

The start of the February 2026 eruption was associated with a very high SO₂ flux (up to 10 kton/day on February 13). These emissions decreased rapidly between February 13 and 15. From February 16 onwards, very low fluxes (< 0.1 kton/day) of SO₂ were measured.

These SO₂ fluxes were used to calculate surface lava flows and are presented in section B of this bulletin.

* Glossary: During rest periods, SO₂ flux at Piton de la Fournaise is below the detection threshold. The SO₂ flux may increase during magma transfer in the shallowest part of the feeding system. During eruptions, it is directly proportional to the amount of lava emitted at the surface.

Phenomenology

February 2026 was marked by a **magmatic intrusion** on February 6-7, 2026 (between 23:31 and 00:05 UTC) that did not reach the surface and **an eruption** that started on February 13 at around 6:00 UTC (10:00 p.m. local time). The first fissures opened on the southern edge of the summit area, and the last one on the **south-south-eastern flank** of the volcano, inside the Enclos Fouqué caldera (see section B for more details). The eruption is still ongoing at the time of writing this bulletin

Summary

The reactivation of the **shallow magma plumbing system** observed since November 2025 continued in February 2026. This pressurization caused the **seismic swarm of February 6-7 2026**, linked to a magma injection from the shallow reservoir towards the surface but which did not reach the surface (magma intrusion).

Following this intrusion, seismic activity continued and **inflation persisted** until February 13, 2026, when a new seismic swarm led to the **second eruption of 2026**; eruption still ongoing at the time of writing this bulletin (see section B for more details)



B. The February 13, 2026 eruption

Eruptive precursors

In the long term

The eruption, which started on February 13, 2026, is part of the ongoing reactivation phase of Piton de la Fournaise, observed since November 2025 (Vigilance phase activated on November 28, 2025; see monthly bulletins for December 2025 and January 2026), characterized by:

- pressurization of the shallow magma reservoir (located between 1.5 and 2 km below the summit) since late November 2025 (indicated by increased seismicity and edifice inflation),
- several magma intrusions (December 5, January 1, February 6–7) and an eruption from January 18 to 20.

In the short term

On **February 13, 2026, at 9:26 a.m. local time** (5:25 a.m. UTC, Figure 9), a seismic swarm was recorded, indicating the rupture of the roof of the shallow magma reservoir and the final propagation of magma towards the surface. Thanks to its automatic alarms, **this seismic crisis enabled OVPF to alert the authorities to the possible imminence of an eruption**. During this crisis, **247 volcano-tectonic (VT) earthquakes** were recorded between 9:25 a.m. and 10:00 a.m. local time. These events were located beneath the summit area (Figure 10).

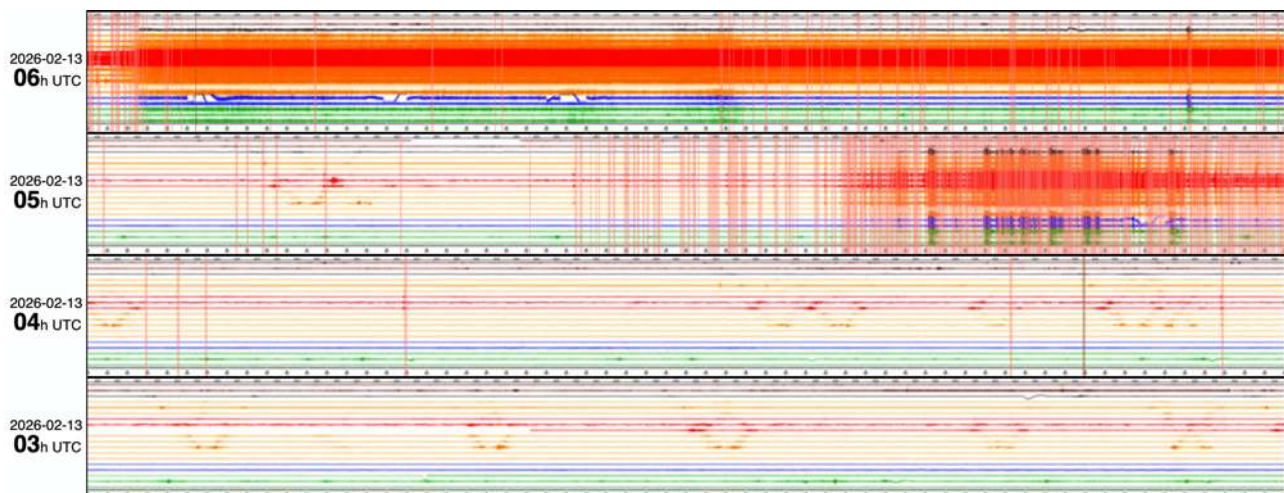


Figure 9: Seismic signals recorded between 3h00 UTC (7h00 local time) and 6h59 UTC (10h59 local time) on February 13, 2026. For each hour (as indicated by the time step on the y-axis), the time is increasing to the right. Each red vertical bar represents an earthquake detected by OVPF-IPGP. Note the appearance of the tremor starting at 6h00 UTC (10h00 local time) (©WebObs/OVPF-IPGP).

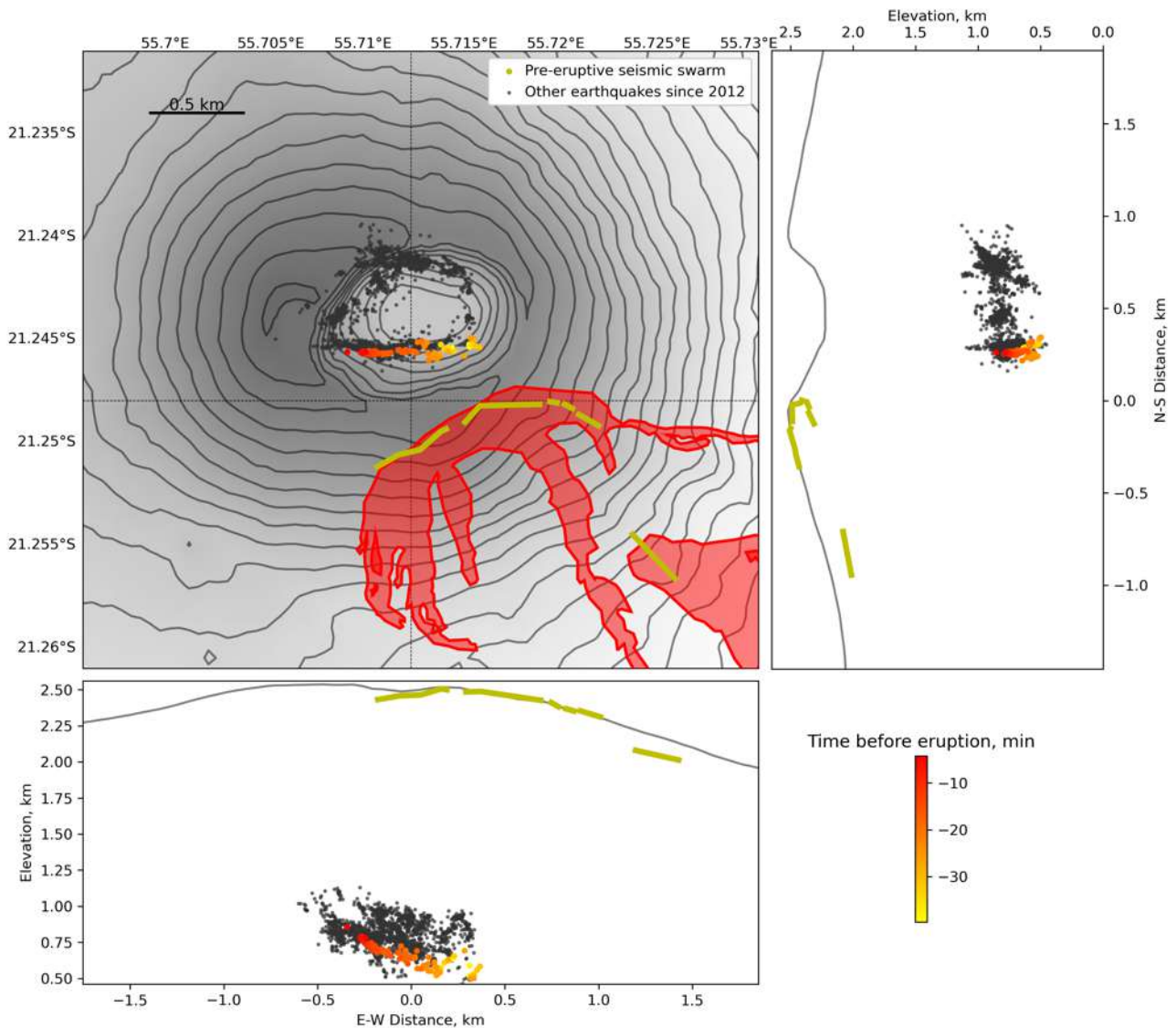


Figure 10: Seismicity recorded during the seismic swarm of February 13, 2026 below Piton de La Fournaise (colored according to the time before the start of the eruption at 6h UTC). Location map (epicenters) and north-south and east-west cross-sections (showing the depth location, hypocenters) of earthquakes detected and relocated by the OVPF-IPGP. The earthquakes in black correspond to a reference catalog of shallow earthquakes since 2012 (©OVPF-IPGP).

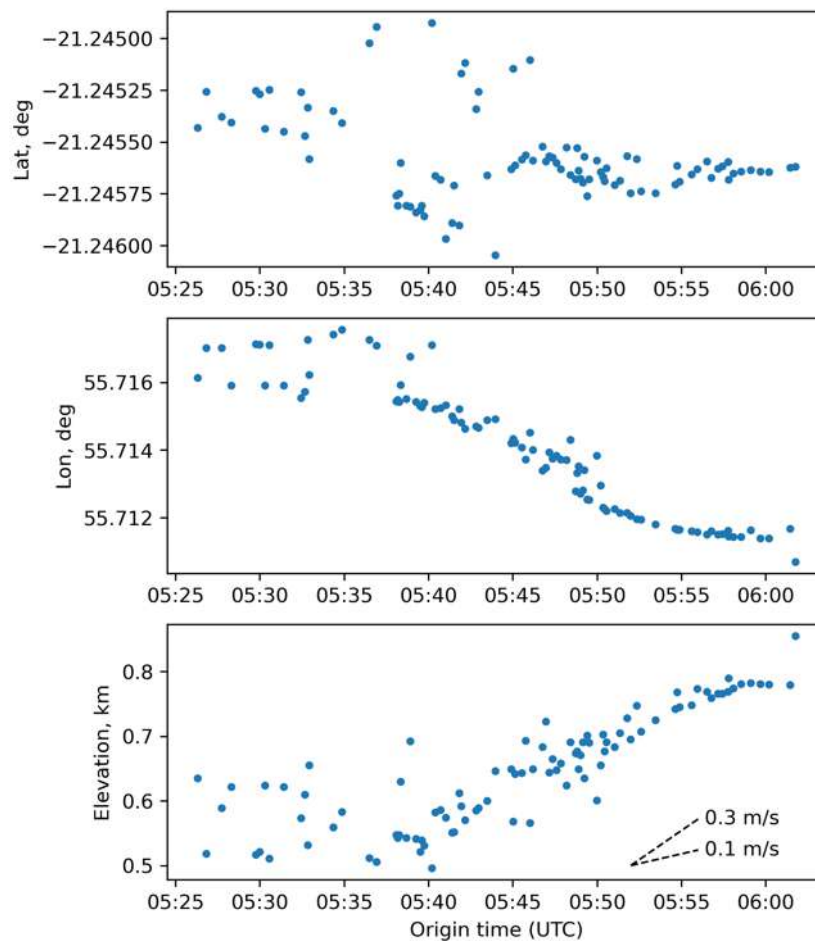


Figure 11: Migration of earthquakes during the pre-eruptive swarm of the February 13, 2026 eruption. The origin time is indicated in hours:minutes UTC on February 13, 2026 (©OVPF-IPGP).

The pre-eruptive seismic swarm was located on the southern part of the annular fault, beneath the southern edge of the Dolomieu crater (Figure 10). As shown in Figure 11, this swarm is associated with a westward and upward migration of seismicity at a speed of between 0.1 and 0.3 m/s. These values are similar to those previously observed at Piton de la Fournaise (Duputel et al., 2019).

The seismic crisis was also accompanied by **rapid deformation**, recorded from 9:40 UTC (5:40 UTC) on the OVPF's permanent GNSS, tiltmeter (Figure 12), and extensometer networks, confirming the rise of magma towards the surface. Vector maps from the tiltmeter network showed **magma migrating towards the southeastern flank of the volcano**.

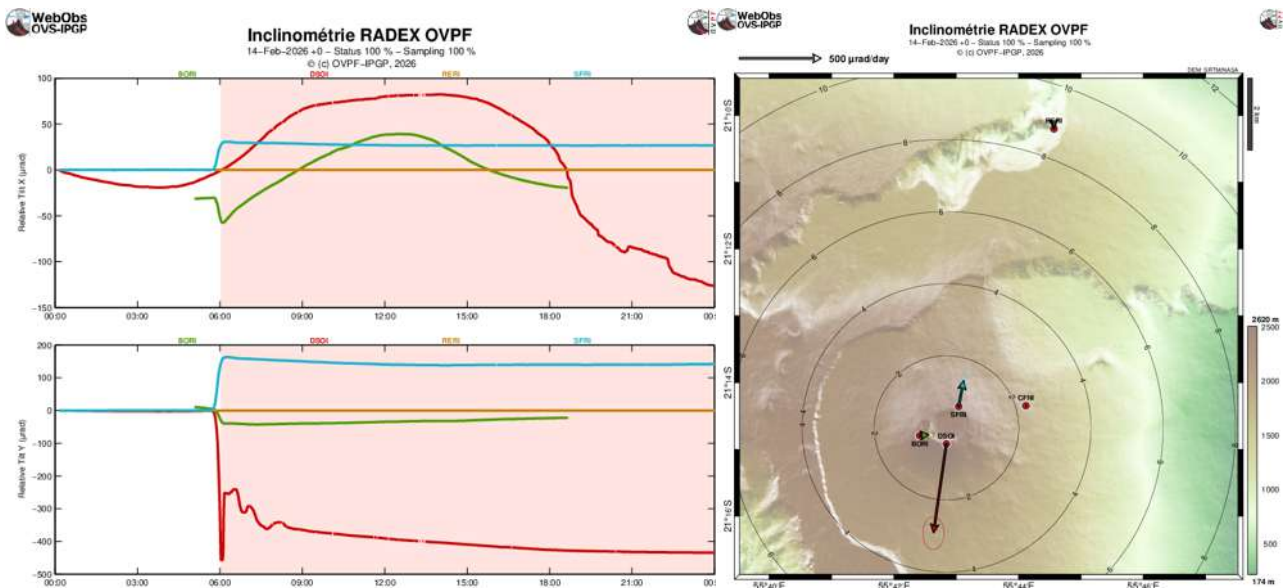


Figure 12: Tiltmeter data from February 13, 2026. Right: slope variations (in microradians) recorded on the tiltmeter network on the X (top) and Y (bottom) components. Left: slope variations represented in vector form (©WebObs/OVPF-IPGP).

Data collected retrospectively on the OVPF GNSS reiteration network (Figure 13) or by radar interferometry (Figure 14) show in greater detail the spatial distribution of surface displacements linked to magma injection. Comparative analysis of these data with those from the permanent GNSS network reveals that, despite taking into account a pre-eruptive phase and a syn-eruptive phase, most of the displacements measured by these two approaches are mainly associated with magma injection towards the surface. Displacements reached around **30 cm on the southern outer edge of the Dolomieu crater and around 40 cm at fissure 4**. These values are relatively low compared to the displacement values recorded during the last eruptions of Piton de la Fournaise and can be explained by strong pre-existing fracturing in this area.

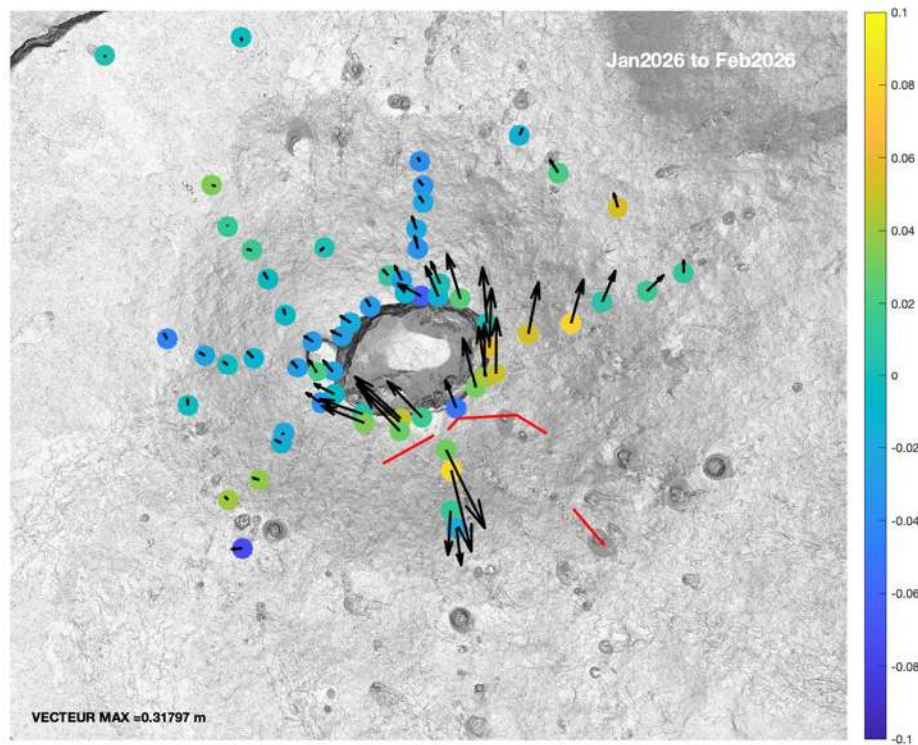


Figure 13: Map of ground displacement (in meters; measured between two GNSS measurement campaigns in January 27-28 and February 18-25, 2026) associated with the injection of magma toward the surface that led to the eruption on February 13, 2026. The vectors represent horizontal displacements (scale given by the numerical value at the bottom left) and the colored circles represent vertical displacements (scale given by the colored bar) (©OVPF/IPGP).

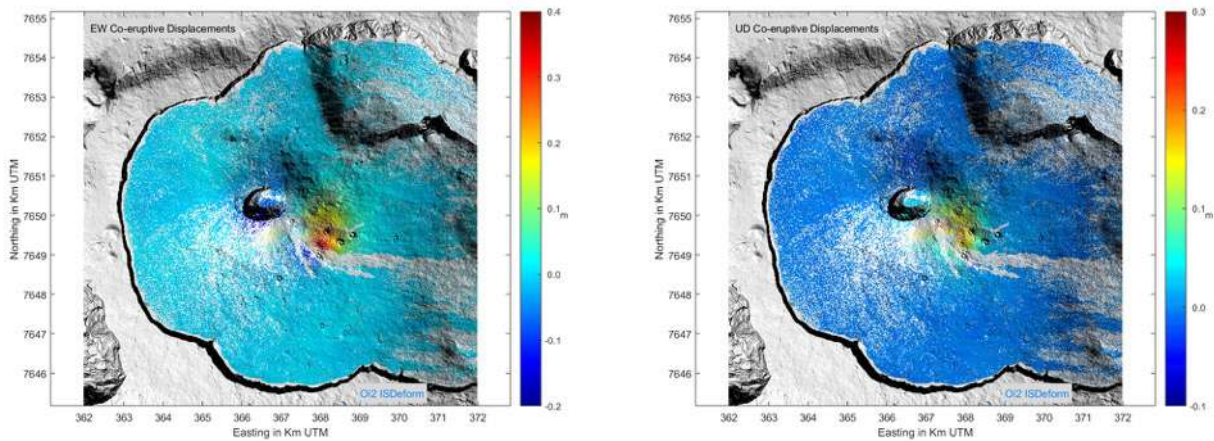


Figure 14: Mapping of east-west (left) and vertical (right) displacements associated with the upward injection of magma that led to the eruption on February 13, inverted from two Sentinel interferograms (one ascending and one descending) (©OI2/ISDeform – OSUL).



At 5:50 a.m. (UTC, 9:50 a.m. local time), the **Jerk alert system** (early eruption warning) recorded a very impulsive signal directed towards the volcano, well above the threshold of 0.1 nm/s^3 ; this indicates an almost certain eruption based on statistics from recent eruptions since 2014 (Beauducel et al., 2025). A few minutes later, the system sent out an automatic telephone message indicating that a magmatic intrusion was indeed taking place. The signal reached a maximum amplitude of 0.83 nm/s^3 (see Figure 15). However, this new 100% automatic alert system, which came into operation during the seismic crisis, only preceded the eruption by 16 minutes on this occasion.

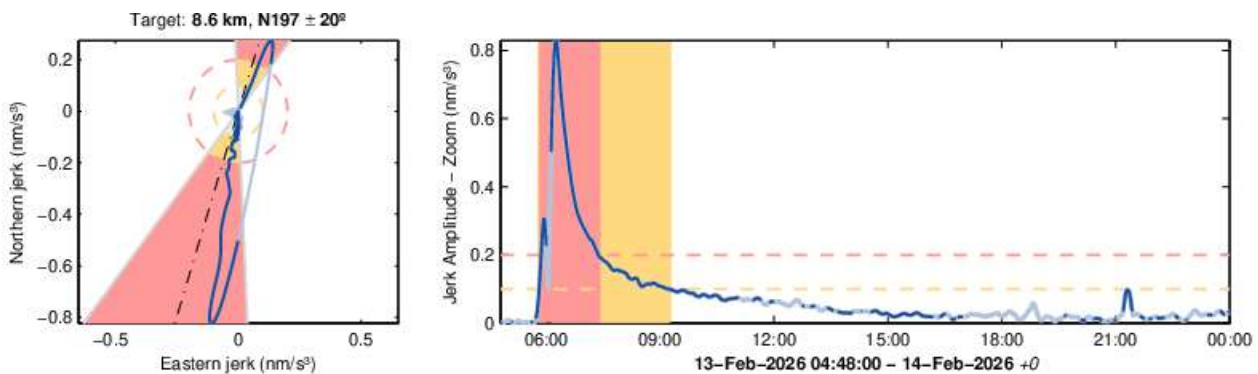


Figure 15: "Jerk" signal associated with the eruption of February 13, 2026, derived from a combination of horizontal acceleration and tilt recorded at the Rivière de l'Est (RER) seismic station, triggered at 9:50 a.m. and with a maximum amplitude of 0.83 nm/s^3 . Left: particle motion showing the trajectory of the transient signal directed toward the summit of the volcano (black dotted line). Right: time signal indicating the peak exceeding the threshold (red dotted line) (©WebObs/OVPF-IPGP).

Co-eruptive signals and observations

The **eruptive tremor**, indicative of magma reaching the surface, appeared at around 10:00 a.m. local time (6:00 a.m. UTC; Figure 9).

Four fissures opened up; three located at the summit, south and southeast of the Dolomieu crater (fissures 1, 2, 3), and a fourth further downstream near Piton Morgabim on the south-southeast flank (fissure 4, see Figures 16, 17, and 18), inside the Enclos Fouqué.

Visual observations and the location of the source of the tremor (seismic signal indicating the emission of lava and gas at the surface; Figure 19) indicate that the eruptive activity, initially centered on the summit area, gradually shifted towards the south-southeast flank with the opening of fissure 4 at around 11:11 a.m. local time (7:11 a.m. UTC; Figure 19).

The opening of fissure 4 was associated with an increase in eruptive tremor between 11:00 a.m. and 1:00 p.m. local time (7:00-9:00 a.m. UTC, Figure 20) at the PVD station, located near the eruptive site.

In detail,

- . Fissure 1: estimated opening around 06:00 UTC (10:00 local time).
- . Fissure 2: opening at 06:03 UTC, then spreading westward, end of activity at 06:27 UTC.
- . Fissure 3: opening at 06:09 UTC, then spreading westward, end of activity at 08:12 UTC
- . Fissure 4: opened at 7:11 UTC then spread south-southeast.

Activity quickly ceased on fissures 2 and 3, focusing instead on fissures 1 and 4. On the morning of February 14, only fissure 4 remained active.



Figure 16: Images of the eruption captured by the IRT webcam located at Piton de Bert. UTC time = Réunion time – 4 hours (©IRT/OVPF-IPGP).



Figure 17: Photo taken from the SAG helicopter during reconnaissance of the eruption site on February 13, 2026, at around 12:50 p.m. local time (©OVPF-IPGP).



Figure 18: Location of eruptive fissures (red segments F1-4: fissures 1-4) and lava flow fronts on February 13, 2026 (red diamonds) (©OVPF-IPGP).

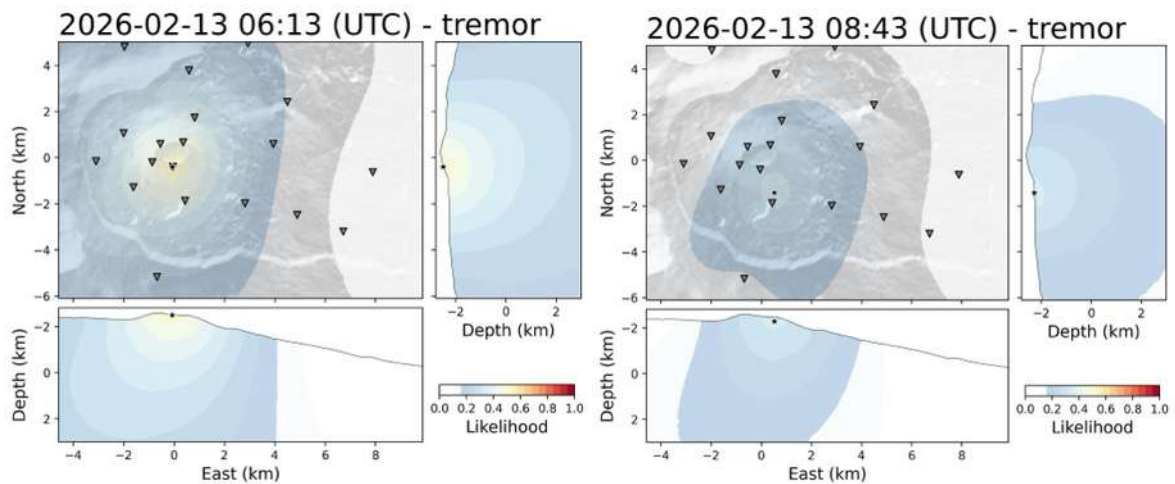


Figure 19: Location of the source of volcanic tremor at the start of the eruption on February 13, 2026. Left: 10:13 a.m. local time (6:13 a.m. UTC); right: 12:43 p.m. local time (8:43 a.m. UTC, right). The star represents the approximate position of the most active eruptive site. UTC time = Réunion time – 4 hours (©OVPF-IPGP).

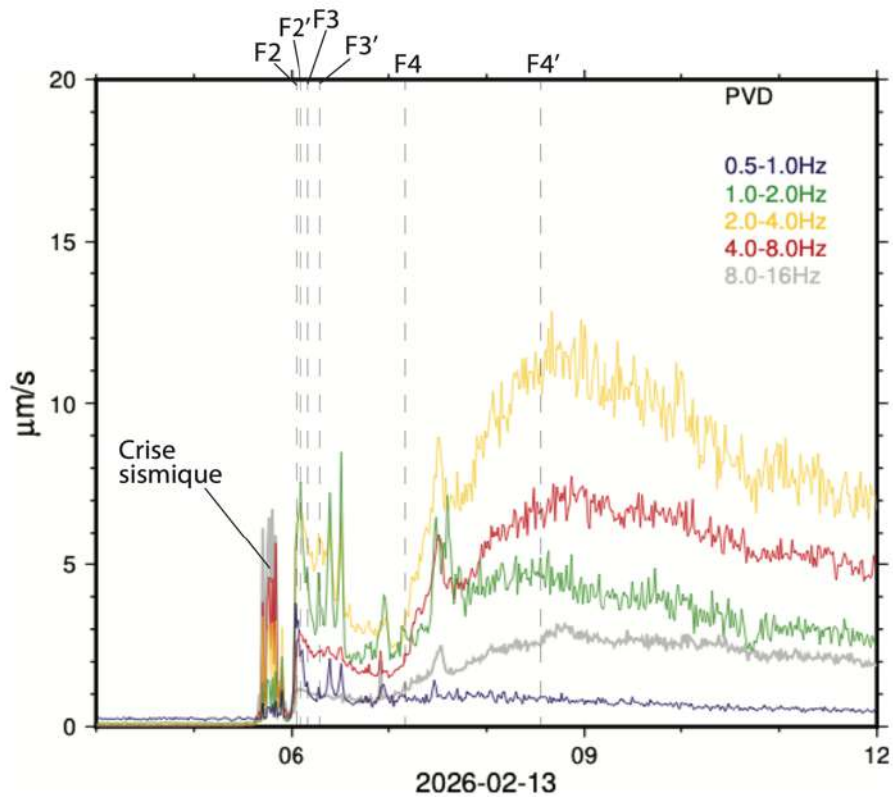


Figure 20: Tremor amplitude measured on the vertical component of the PVD seismic station located near the F4 eruptive fissure (see Figures 17 and 18) and filtered in different frequency bands. F2, F3, and F4 indicate the beginning of the opening of fissures F2, F3, and F4, while F2', F3', and F4' indicate the end of the opening of these fissures (©OVPF-IPGP).

It should be noted that **the time between the start of the seismic crisis and the start of the eruption was extremely short** (approximately 35 minutes). However, this duration is **typical of an eruption occurring near the summit** (Figure 21). As the magma reservoir is located beneath the summit area, the magma travels a relatively short distance (less than 2 km). Furthermore, the magma injection takes place in a highly fractured environment, facilitating its propagation. Eruptions further away from the summit are generally preceded by longer seismic crises (distance-duration relationship illustrated in Figure 21).

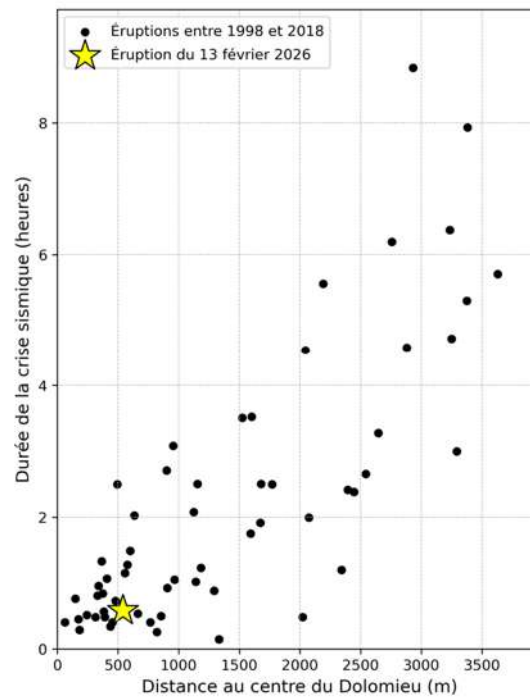


Figure 21: Duration of the pre-eruptive seismic crisis as a function of the distance of the first fissures opening at the start of eruptions (relative to the center of Dolomieu) observed at Piton de la Fournaise for the period 1998-2018. The case of February 13, 2026 is represented by a yellow star (©OVPF-IPGP).

Figure 22 shows the temporal evolution of the amplitude of the eruptive tremor between February 13 and 28, 2026. After the initial increase in tremor when the various eruptive fissures opened (Figure 20), a gradual decrease in its amplitude was observed until February 22. Since then, the tremor has been relatively stable with a slight long-term upward trend. This temporal evolution of the tremor amplitude is similar to the evolution of the rates estimated from satellite data (Figure 23) and from SO₂ fluxes (Figure 24).

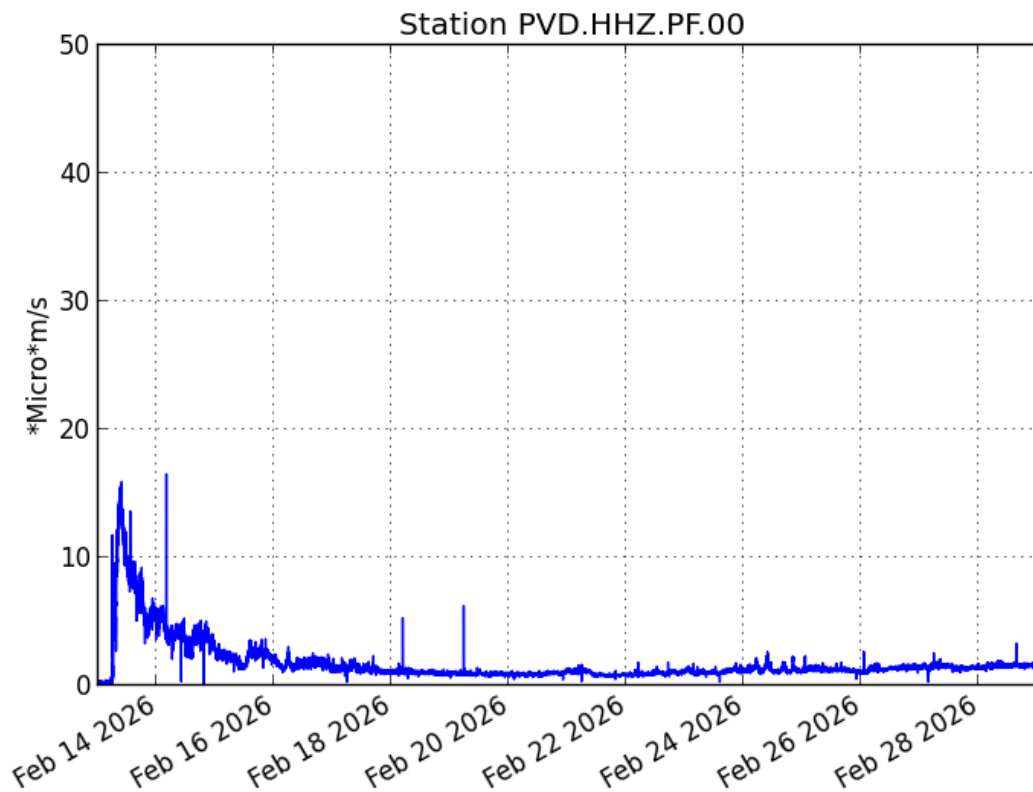


Figure 22: Evolution of tremor amplitude (indicator of lava and gas emissions at the surface) between February 13, 2026, and February 28, 2026, at the PVD seismic station located near the eruption (©WebObs/OVPP-IPGP).

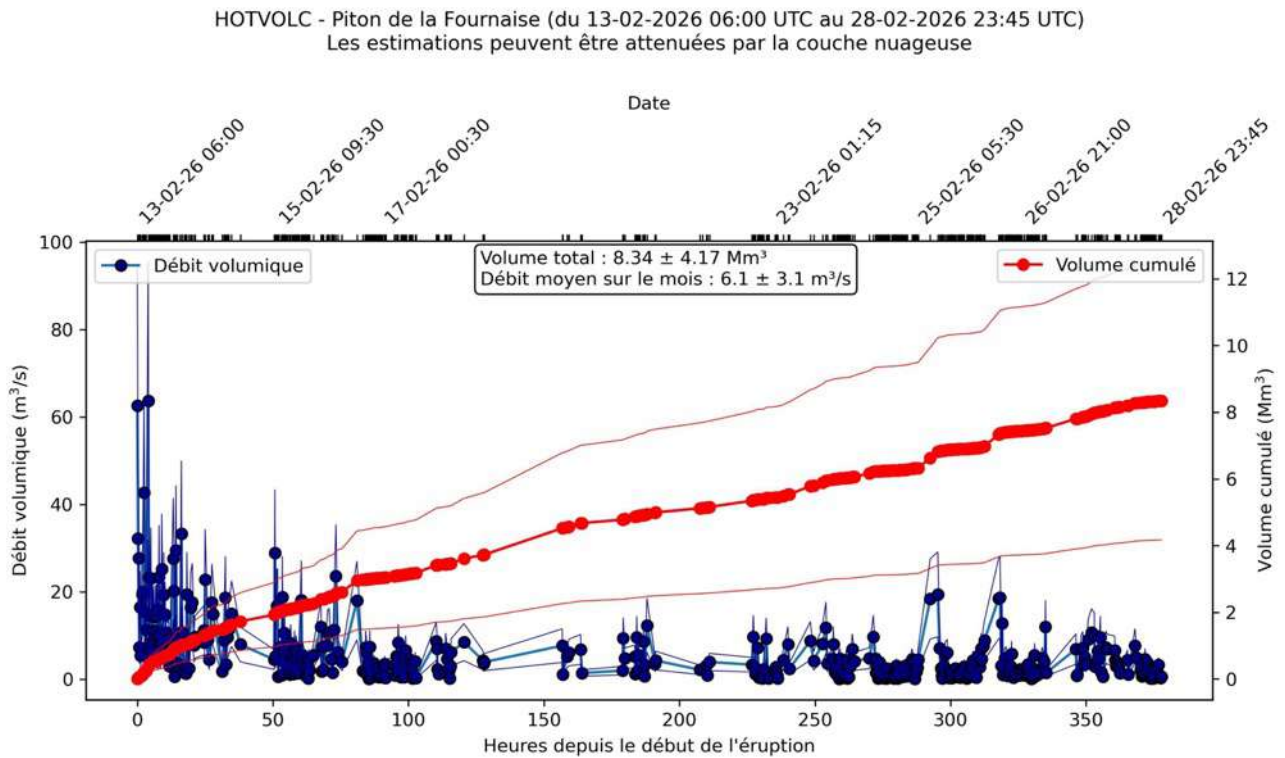


Figure 23: Estimated cumulative lava volume emitted at the surface (Mm^3 , in red) and lava flow rates at the surface (m^3/s , in blue) based on satellite data from the HOTVOLC platform between February 13 and February 28, 2026 (©OPGC-Clermont Auvergne University).

Lava discharge rates, estimated from satellite data via the HOTVOLC (OPGC – Clermont Auvergne University, Figure 23) and MIROVA (University of Turin, Figure 24) showed values reaching **up to $63 \text{ m}^3/\text{sec}$** during the first hours of the eruption, then declining as the activity of the first fissures ceased. From February 16, average flow rates were **$< 20 \text{ m}^3/\text{sec}$** and most of the time between 1 and $10 \text{ m}^3/\text{sec}$ (Figure 23). It should be noted that, depending on cloud cover, these estimates can vary rapidly and become zero in the event of total cloud cover.

The lava discharge, estimated from satellite thermal data, are broadly consistent with those calculated from SO_2 fluxes measured by OVPF NOVAC stations installed around Enclos Fouqué (Figure 24). The differences observed are related to the geometry of the plume and meteorological conditions.

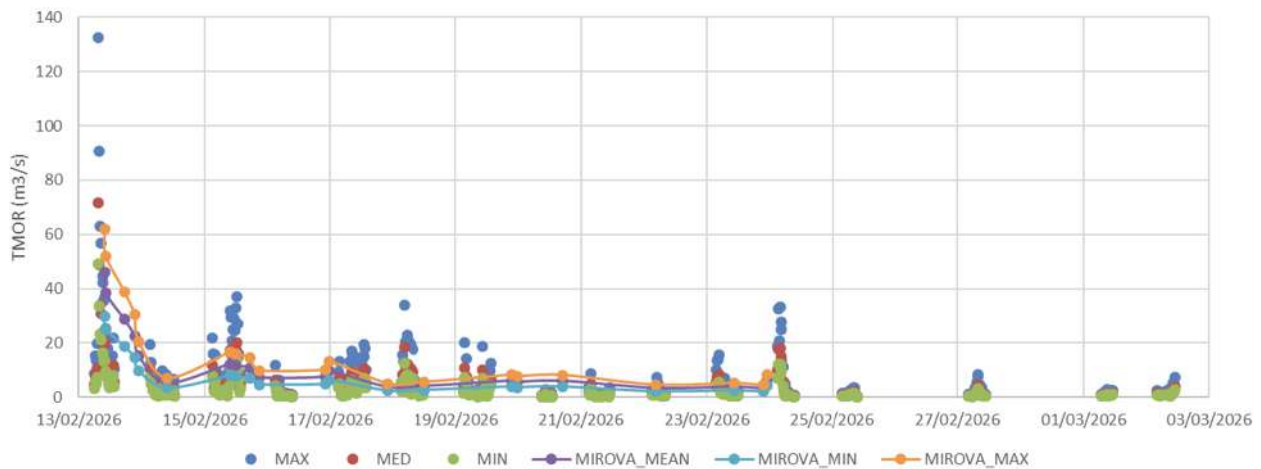


Figure 24: Estimation of lava discharge rates (m^3/s) based on SO_2 fluxes recorded on the OVPF's NOVAC network (points; blue: maximum values, red: average values, green: minimum values) and compared with estimates made using satellite data from the MIROVA platform (University of Turin) (solid lines; orange: maximum values, purple: average values, cyan: minimum values) between February 13 and March 3, 2026 (©OVPF-IPGP-OSUL).

Estimating lava discharges makes it possible to monitor the volume of lava emitted at the surface; between February 13 and 28, 2026, approximately **8 million m^3 of lava** was emitted at the surface (Figure 23).

From the beginning of the eruption, the paths of the lava flows were modeled using the DOWNFLOWGO model (LMV-Université Clermont Auvergne) and were communicated to the «*Etat-Major de Zone et de Protection Civile de l'Océan Indien*» (EMZPCOI) during crisis management. The map shows that numerical simulations (Figure 25) accurately predicted the stopping point of the flow front for flow rates $< 20 m^3/sec$.

From February 15 onwards, as the flow rate decreased, the lava front stopped in Grand Brûlé at an altitude of 660 m, approximately 2.6 km from National Road 2 (Figure 26).

Figure 27 shows the progress of the various lava flows as of February 26, 2026.



Carte de simulation DOWNFLOWGO pour l'éruption en cours

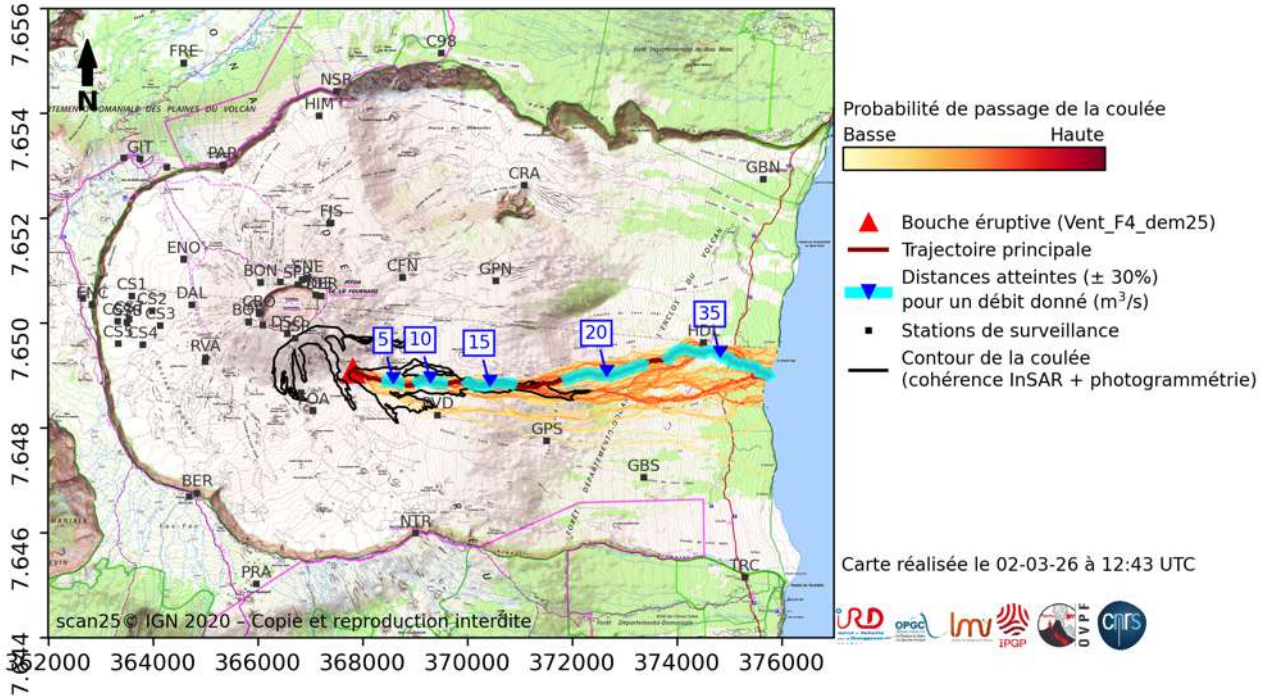


Figure 25: Numerical simulations of probable lava flow inundation paths for the February 13, 2026 eruption (following the protocol described in Harris et al. 2019). The inundation area is computed for 10000 iterations from the initial vent location with vertical elevation noise of 2 m via the DOWNFLOW model (Favalli et al. 2005). Yellow to red lines represent the frequency of lava paths from low (yellow) to high (red). The line of steepest descent (LoSD) is shown in red. Blue arrows represent the location at which the lava could extend along the LoSD for given effusion rates (numbers are in m^3/s) as computed using the FLOWGO model (Harris and Rowland 2001; Chevrel et al. 2018). The light blue lines represent a 30% uncertainty in the distance. The black outline shows the contour of the lava flow as of February 26, 2026 (©OPGC-LMV-OVPF-IPGP).

Références:

- . Chevrel MO, Labroquere J, Harris AJL, Rowland SK (2018) PyFLOWGO: An Open-Source Platform for Simulation of Channelized Lava Thermo-Rheological Properties. *Comput. Geosci.* 111: 167–80. <https://doi.org/10.1016/j.cageo.2017.11.009>
- . Favalli M, Pareschi MT, Neri A, Isola I (2005) Forecasting Lava Flow Paths by a Stochastic Approach. *Geophys. Res. Lett.* 32(3): 1–4. <https://doi.org/10.1029/2004GL021718>
- . Harris AJL, Chevrel MO, Coppola D, Ramsey MS, Hrysiwicz A, Thivet S, Villeneuve N et al. (2019) Validation of an Integrated Satellite-data-driven Response to an Effusive Crisis: The April–May 2018 Eruption of Piton de La Fournaise. *Ann. Geophys.* 61. <https://doi.org/10.4401/ag-7972>
- . Harris AJL, Rowland SK (2001) FLOWGO: A Kinematic Thermo-Rheological Model for Lava Flowing in a Channel. *Bull. Volcanol.* 63: 20–44. <https://doi.org/10.1007/s004450000120>

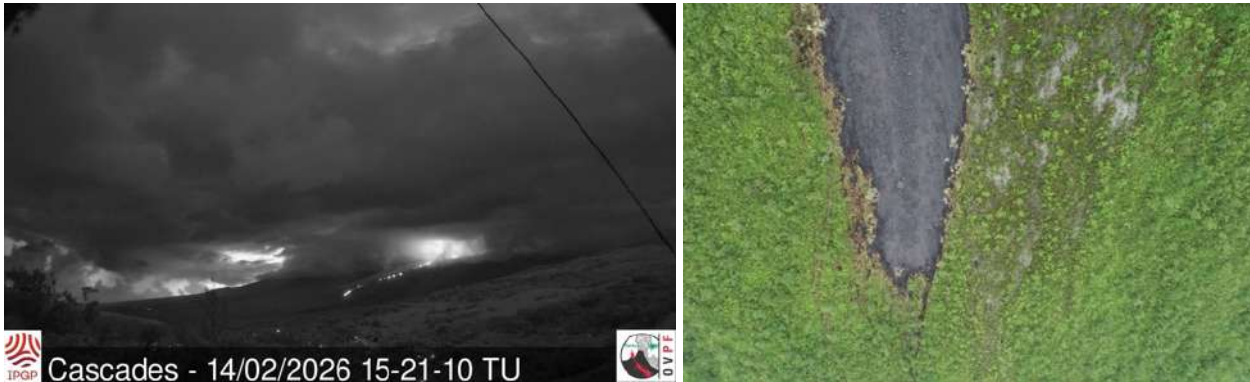


Figure 26: Images of the lava flow. Left: from the OVPF webcam located at Piton des Cascades on February 14, 2026, at 3:21 p.m. UTC (7:21 p.m. local time). Right: February 15, 2026, at 2:15 p.m. (©OVPF-IPGP).

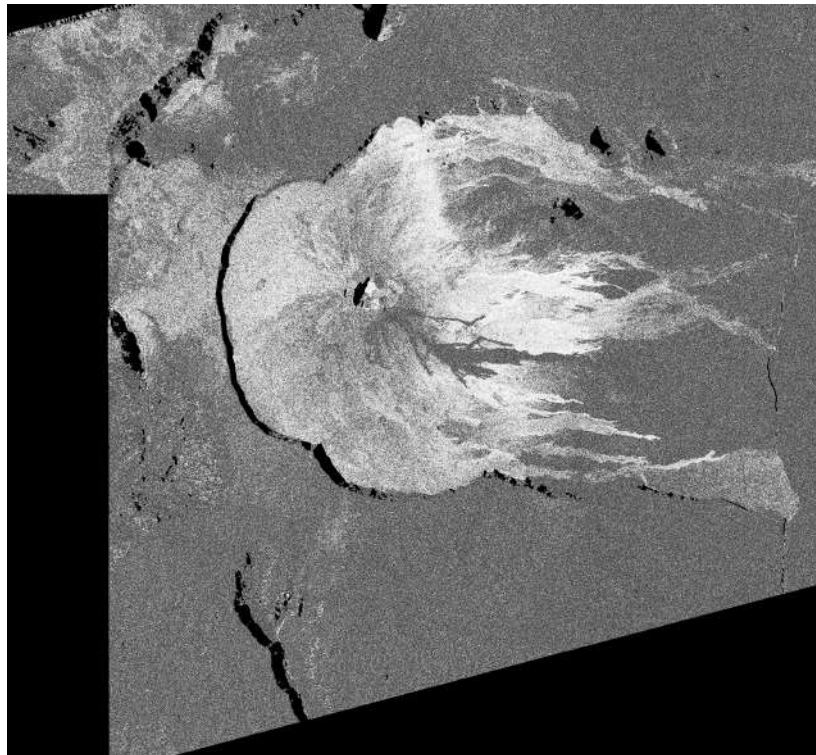


Figure 27: Coherence map calculated from the Sentinel-1 Stripmap Ascending interferogram covering the period from February 8, 2026, to February 26, 2026. The various branches of the lava flow emitted by the eruption are visible (dark areas = low coherence) on the southern and southeastern flanks of the terminal cone. The flow extends eastward into the Grandes Pentes. It eventually becomes indistinguishable from the surrounding vegetation, which is also characterized by low coherence (©OI2/ISDeform – OSUL).



Figure 28: Various images of the eruptive site showing the evolution of the volcanic cone. Left: image taken from the southeast of the cone on February 17, 2026. Middle: image taken from the west of the cone on February 18, 2026. Right: image taken from the north of the cone on February 27, 2026 (©OVPF-IPGP).

At the end of February, only one eruptive site remained active on the south-southeastern flank of the volcano, with fountains still visible. A cone was still being built up by the gradual accumulation of lava projections (Figure 28). On February 27, the cone reached a height of 19 meters on its northeast edge, and the highest lava projections rose about 20 meters above its summit. With the lateral closure of the cone, significant lava tunnel activity developed downstream of the cone. The resurgence of the lava flow and the active aerial parts of the lava flow were concentrated downstream of the eruptive site and upstream of the Grandes Pentes break, where the lava field widened and thickened.

At the time of writing, the eruption **is still on-going and a renew of summit inflation is recorded**; the continuation of this eruption will therefore be discussed in the next monthly bulletin.



C. Seismic activity on La Réunion and in the Indian Ocean basin

Local and regional seismicity

In February 2026, the OVPF-IPGP recorded:

- 41 local earthquakes (below the island, within a radius of 200 km around the island, Figures 29 and 30);
- 1 regional earthquake (in the Indian Ocean basin).

In February 2026, the OVPF-IPGP detected **41 local earthquakes** located mainly below the *Roche Ecrite* area, but also to the east of *Salazie* and below *Grand Etang* (Figure 30). Most of these earthquakes have **magnitude less than 1** and are difficult to locate accurately. These earthquakes were located between **10 km and 25 km depth in oceanic lithosphere** on which was built the volcanic edifice at the origin of La Réunion island.

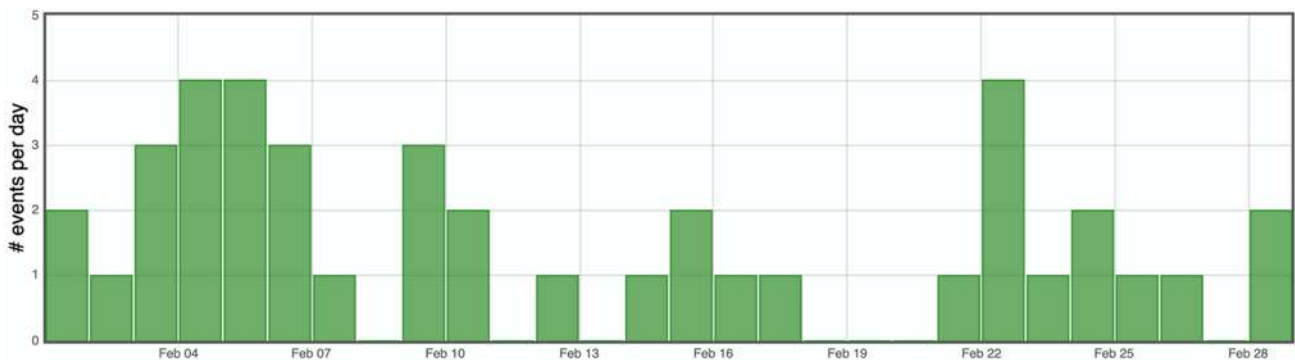
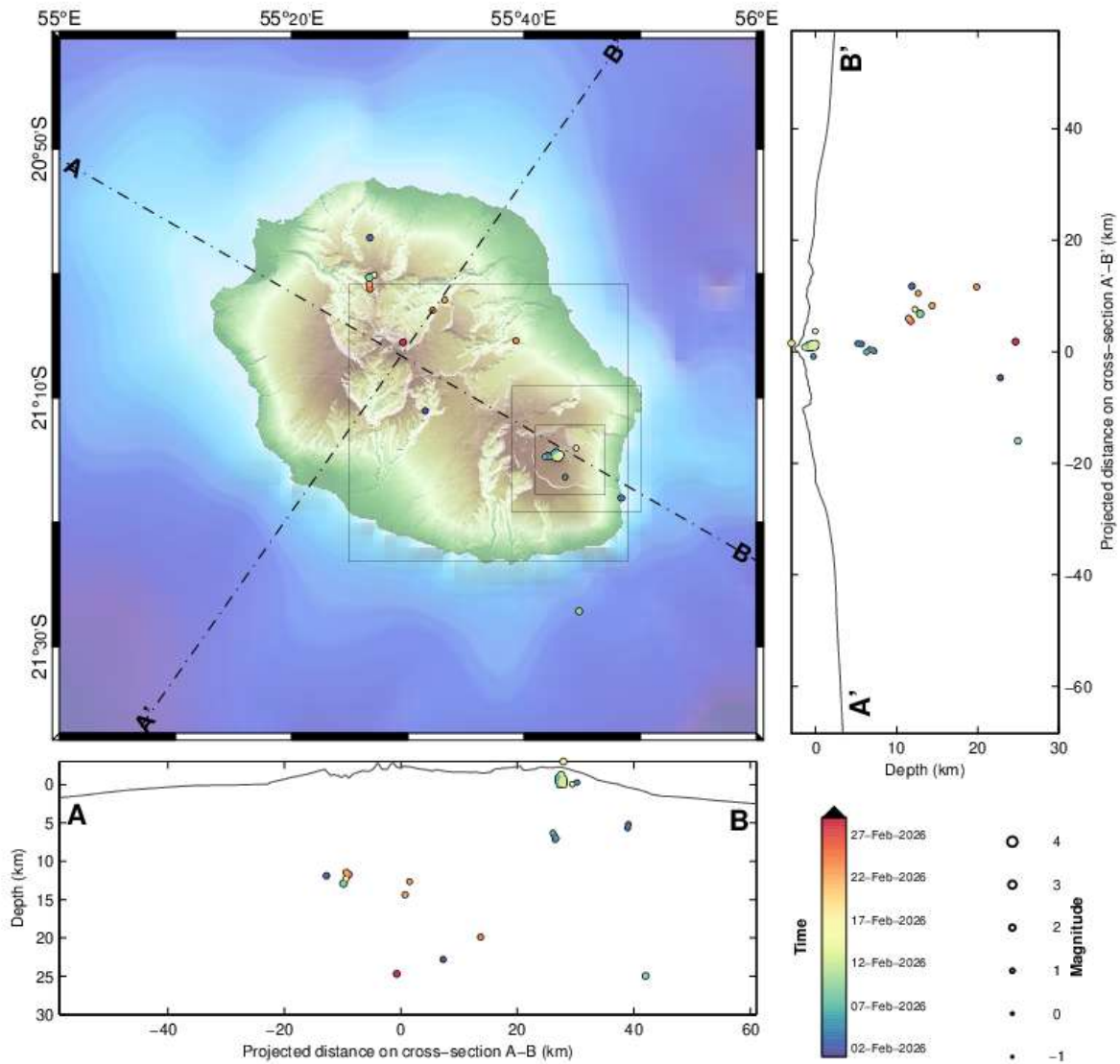


Figure 29: Number of local earthquakes (La Réunion island) per day recorded in February 2026 (©WebObs/OVPF-IPGP).



La Réunion
© OVPF-IPGP, 2026



Filters: MAG ∈ [-1,6]; DEP ∈ [-3,30];

From: 01-Feb-2026 00:00
To: 01-Mar-2026 00:00

Total events = 122
Magnitude: min -0.3 - max 2.0
Types:
Local (13),

Profond (7),
Sommital (102),

Figure 30: Seismicity below La Réunion in February 2026. Location map (epicenters) and north-west – south-east and south-west – north-east cross-sections (hypocenters) of earthquakes as recorded by OVPF-IPGP. Only localizable earthquakes are shown on the map (©WebObs/OVPF-IPGP).



Seismic-volcano activity in Mayotte

The « REseau de surveillance VOlcanologique et SIsfmologique de MAyotte (REVOSIMA) » is the structure in charge of the volcano and seismic monitoring of Mayotte. IPGP and BRGM coordinate and manage REVOSIMA. Operational monitoring of seismic-volcanic activity is carried out by IPGP (OVPF), under the joint responsibility of BRGM and in close association with IFREMER and CNRS. REVOSIMA is supported by a scientific and technical partnership. The REVOSIMA consortium: IPGP and Université Paris Cité, BRGM, IFREMER, CNRS, BCSF-RéNaSS, ITES and Université de Strasbourg, IGN, ENS, SHOM, TAAF, CNES, Université Grenoble Alpes and ISTerre, Université Clermont Auvergne, LMV and OPGC, Université de La Réunion, Université Paul Sabatier, Toulouse and GET-OMP, Université de la Rochelle, Université de Bretagne Occidentale, IRD and collaborators.

All information on the REVOSIMA and the activity in Mayotte can be found on the dedicated webpages:

- <https://www.ipgp.fr/observation/infrastructures-nationales-hebergees/revosima/>
- <https://www.ipgp.fr/actualites-du-revosima/>
- <https://www.facebook.com/ReseauVolcanoSismoMayotte/>
- <https://bsky.app/profile/revosima.bsky.social>

March 4, 2026
OVPF-IPGP Director



D. Appendix

Definition of Volcanic Alert Levels for Piton de la Fournaise

from *disposition spécifique « Volcan Piton de la Fournaise » - arrêté n°2242*- Emergency plan set up by the department responsible for the protection of the population in the event of unrest or activity of the Piton de la Fournaise

• **“Vigilance”**: possible eruption in medium term (a few days or weeks) or presence of risks on the sector (rockfalls, increase of gas emissions, still hot lava flows...).

Access to the Enclos Fouqué caldera and to the summit volcano are allowed with restrictions.

• **“Alert 1”**: probable or imminent eruption.

Access to the Enclos Fouqué caldera and to the summit are closed and prohibited.

• **“Alert 2”**: ongoing eruption.

Alert 2-1: ongoing eruption inside the Enclos Fouqué caldera without threat to the safety of people, property or the environment

Alert 2-2: ongoing eruption inside the Enclos Fouqué caldera with direct or indirect threat to the safety of people, property or the environment.

Access to the Enclos Fouqué caldera and to the summit are closed and prohibited. For Alert 2-2, evacuation of the people and vehicles depending on the issues.

• **“Alert 2-3”**: ongoing eruption outside the Enclos Fouqué caldera with threat to the safety of people, property or the environment.

Access to the Enclos Fouqué caldera and to the summit are closed and prohibited. Evacuation of the people and vehicles depending on the issues.

• **“Sauvegarde”**: end of eruption.

Evaluation of a partial reopening of the Enclos Fouqué caldera access.



References

- Altamimi, Z., Rebischung, P., Collilieux, X., Métivier, L., & Chanard, K. (2023), ITRF2020: an augmented reference frame refining the modeling of nonlinear station motions, *Journal of Geodesy*, 97(5), 47. <https://link.springer.com/article/10.1007/s00190-023-01738-w>
- Arellano, S., Galle, B., Apaza, F., Avard, G., Barrington, C., Bobrowski, N., ... Yalire, M. (2020), Synoptic analysis of a decade of daily measurements of SO₂ emission in the troposphere from volcanoes of the global ground-based Network for Observation of Volcanic and Atmospheric Change, *Earth System Science Data Discussions*, 2020, 1-3
- Beauducel, F., Roult, G., Ferrazzini, V., Peltier, A., Jousset, P., Boissier, P., Villeneuve, N. (2025), Jerk, a promising tool for early warning of volcanic eruptions. *Nat Commun* 16, 11418, <https://doi.org/10.1038/s41467-025-66256-z>
- Bénard, B., Di Muro, A., Liuzzo, M., Gurrieri, S., Boissier, P., Brunet, C. et al. (2023), Seasonal environmental controls on soil CO₂ dynamics at a high CO₂ flux sites (Piton de la Fournaise and Mayotte volcanoes), *Journal of Geophysical Research: Biogeosciences*, 128(6), e2023JG007409
- Bertiger, W., Bar-Sever, Y., Dorsey, A., Haines, B., Harvey, N., Hemberger, D., ... & Willis, P. (2020), GipsyX/RTGx, a new tool set for space geodetic operations and research, *Advances in space research*, 66(3), 469-489
- Bouidoire, G. (2017), Architecture et dynamique des systèmes magmatiques associés aux volcans basaltiques : exemple du Piton de la Fournaise. *Volcanologie*, Université de la Réunion, 2017. Français. (NNT : 2017LARE0022). (tel-01902958)
- Chevrel, MO., Labroquere, J., Harris, AJL, Rowland, SK (2018), PyFLOWGO: An Open-Source Platform for Simulation of Channelized Lava Thermo-Rheological Properties. *Comput. Geosci.* 111: 167–80. <https://doi.org/10.1016/j.cageo.2017.11.009>
- Duputel, Z., Lengliné, O., Ferrazzini, V. (2019), Constraining Spatiotemporal Characteristics of Magma Migration at Piton De La Fournaise Volcano From Pre-eruptive Seismicity, *Geophys. Res. Lett.* 46: 119-127, <https://doi.org/10.1029/2018GL080895>
- Favalli, M., Pareschi, MT., Neri, A., Isola, I. (2005), Forecasting Lava Flow Paths by a Stochastic Approach, *Geophys. Res. Lett.* 32(3): 1–4. <https://doi.org/10.1029/2004GL021718>
- Harris, AJL., Chevrel, MO., Coppola, D., Ramsey, MS., Hrysiwicz, A., Thivet, S., Villeneuve, N. et al. (2019), Validation of an Integrated Satellite-data-driven Response to an Effusive Crisis: The April–May 2018 Eruption of Piton de La Fournaise, *Ann. Geophys.* 61, <https://doi.org/10.4401/ag-7972>
- Harris, AJL., Rowland, SK. (2001), FLOWGO: A Kinematic Thermo-Rheological Model for Lava Flowing in a Channel. *Bull. Volcanol.* 63: 20–44. <https://doi.org/10.1007/s004450000120>
- Lomax, A., Virieux, J., Volant, P., & Berge-Thierry, C. (2000), Probabilistic earthquake location in 3D and layered models. In C. H. Thurber & N. Rabinowitz (Eds.), *Advances in Seismic Event Location, Modern Approaches in Geophysics* (pp. 101–134). Springer, Dordrecht, Netherlands
- Murphy, D., Bertiger, W., Hemberger, D., Komanduru, A., Peidou, A., Ries, P., & Sibthorpe, A. (2024), Jet Propulsion Laboratory Analysis Center Technical Report 2024. In R. Dach & E. Bockmann (Eds.), *International GNSS Service Technical Report 2024 (IGS Annual Report)*, IGS Central Bureau and University of Bern; Bern Open Publishing. <https://doi.org/10.48350/191991>
- Rebischung, P., Altamimi, Z., Métivier, L. et al. (2024), Analysis of the IGS contribution to ITRF2020, *J Geod* 98, 49. <https://doi.org/10.1007/s00190-024-01870-1>
- SeisComP (2024), SeisComP 6 – Earthquake Monitoring Software, <https://www.seiscomp>

